



# AusArray: uncovering major crustal features using passive seismic data

**Alexei Gorbatov**

Geoscience Australia  
GPO Box 378, Symonston ACT2601  
Alexei.Gorbatov@ga.gov.au

**Andrew Medlin**

Geoscience Australia  
GPO Box 378, Symonston ACT2601  
Andrew.Medlin@ga.gov.au

**Michael P. Doublier**

Geoscience Australia  
GPO Box 378, Symonston ACT2601  
Michael.Doublier@ga.gov.au

**Karol Czarnota**

Geoscience Australia  
GPO Box 378, Symonston ACT2601  
Karol.Czarnota@ga.gov.au

**Tanya Fomin**

Geoscience Australia  
GPO Box 378, Symonston ACT2601  
Tanya.Fomin@ga.gov.au

**Paul Henson**

Geoscience Australia  
GPO Box 378, Symonston ACT2601  
Paul.Henson@ga.gov.au

**Brian L.N. Kennett**

RSES, ANU, Canberra ACT2000  
Brian.Kennett@anu.edu.au

## SUMMARY

It is generally accepted that improvements in mineral exploration are required to meet the rising demand for minerals associated with a transition to lower carbon energy sources. There is growing consensus in mineral exploration that the distribution of fertile mineral camps is controlled by major lithospheric structures yet there is a paucity of case studies with adequately distributed datasets to test this view. Here, we test the relationships between variations in the Mohorovičić discontinuity (Moho) and iron oxide-copper-gold and sediment-hosted mineral deposits in the regions between the Arunta and Mount Isa Provinces. We primarily utilise datasets from the Australian passive seismic array (AusArray) and pre-existing academic seismometer deployments supplemented by deep reflection seismic profiles. The 55–70 km seismometer interstation distance provides almost continuous imaging of the Moho interface using back-projected receiver functions. We observe the Moho surface undulates at depths of ~35 to ~50 km, reflecting the complex regional tectonic framework of the area. Sharp steps are observed associated with major crustal boundaries such as the Willowra Suture and the Cork Fault, while other changes are more gradual but on the first order correspond to lithospheric thickness variations. Inspection of the Moho surface and the spatial distribution of base metal deposits suggests that significant deposits (>2 Mt) are distributed along the edges of second-order north–south to northeast–southwest-trending thicker crustal blocks. Our results indicate that passive seismic methods are a powerful tool to generate continuous datasets across large regions from which important architectural features can be identified to support exploration under cover in frontier regions. Higher-resolution seismic surveys would be useful to link these structures with mineral camps in the near surface.

**Key words:** AusArray, passive seismic, Moho, crustal structures, mineral deposits

## INTRODUCTION

To improve exploration success undercover, the UNCOVER initiative identified high-resolution 3D seismic velocity characterisation of the Australian plate as a high priority. To

achieve this goal, the Australian Government and academia have united around the AusArray initiative. The aim is to obtain a national half-degree data coverage and an updatable 3D national velocity model, which grows in resolution as more data become available. AusArray combines data collected from the Australian National Seismological Network, multiple academic transportable arrays (supported by AuScope and individual grants) and the Seismometers in Schools program. The Australian Government's Exploring for the Future program has enabled the unification of these datasets and a doubling of the national rate of data acquisition. Extensive quality control checks have been applied across the AusArray dataset to improve the robustness of subsequent Australian continent imaging.

The receiver function imaging technique (RF) allows the mapping of crust and upper mantle interfaces associated with sharp changes in seismic wave propagation properties. The most well-known interface is the Mohorovičić discontinuity (Moho), which separates the crust and the upper mantle. Seismic waves, which arrive at a seismic station, convert modes of propagation and reflect at the discontinuity forming a unique fan shape pattern that can be used to generate an image of the interface that is similar to images generated from active seismic reflection profiles. Spacing between seismic stations defines the spatial resolution of the image and the frequency of seismic signal controls the vertical resolution (a few kilometres at >~1Hz). This resolution is sufficient to confidently track the shape of the Australian Moho discontinuity (Salmon *et al.* 2013).

A robust understanding of the Moho provides core information for gravimetric modelling and important constraints on the nature and distribution of crustal blocks, and their boundaries, utilised in mineral and energy system assessments (e.g. Skirrow *et al.*, 2019). Given the growing volume of seismic data (Figure 1) and constant advances in techniques for data processing and inversion, there is a growing need for an updatable Moho discontinuity model of Australia. As part of the Exploring for the Future program, Geoscience Australia (GA) developed standardized workflows to treat all datasets in a consistent manner (Hassan 2020). We apply this workflow systematically to datasets when data processing technique are modified or new data is acquired. Our approach reduces discrepancies introduced by differences between processing methods and human factors and thereby provides standardised and repeatable constraints on the Moho.

Here we apply our standardized approach of mapping the Moho over the Alice Springs to Mount Isa area mostly based on RF analysis. These results are complemented by reflection results from the Exploring for the Future program and supplemented with results previously published by academia.

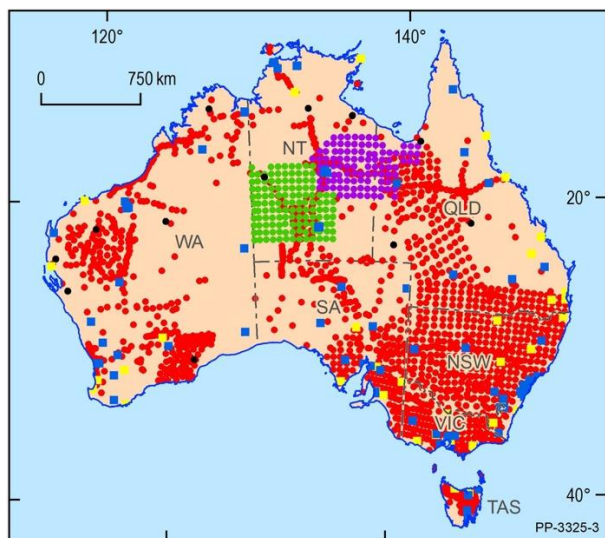


**Figure 1. Map of passive seismic stations recompiled by Geoscience Australia. Results from Exploring for the Future phase 1 and 2 deployments are presented in this study.**

### METHOD

Our RF calculation workflow follows the approach by Ammon (1991) with extensive pre-processing of raw data to remove noisy records and the influence of sedimentary basins (e.g. Tkalčić *et al.*, 2011, Yu *et al.*, 2015). Resulting records were analysed using the H-K technique of Zhu and Kanamori (2000) to estimate the depth to the Moho interface and as a support to migrating image analysis (Kosarev *et al.*, 1999).

We combined five classes of Moho depth estimates to construct the shape of the Moho (Table 1). These include both our new results and legacy active and passive seismic recordings.

Reflection profiling was initially carried out in southern Queensland with explosive sources, but most lines in the region have been collected using vibrator sources. The Moho results for reflection lines are extracted at approximately 20 km intervals based on an interpretation of the base of crustal reflectivity. Such measurements are made on time-migrated record sections (e.g. Kennett *et al.*, 2016) or, for more recent surveys, from the field stacks. Depth conversion utilised a simple approximation of a constant conversion velocity of 6 km/s. This approach has been calibrated in a number of locations in Australia against other methods, and works well with differences typically less than 1–2 km. In areas where

sedimentary cover is >4 km thick, Moho depths are likely to be overestimated. A complementary procedure that avoids problems in areas with complex near-surface conditions exploits the autocorrelation of passive seismic signals, for either continuous data or teleseismic arrivals (Qashqai *et al.*, 2019).

To construct the Moho surface, the weighted contributions from all the datasets are combined, using the distance from each observation point to the desired location. Contributions from far stations are negligible, but close ones contribute strongly according to their assigned weighting (Kennett, 2019). There is a contribution from both the relative weight assigned to the dataset and for the particular observation. These factors are multiplied to give the actual weight applied to the distance term that has Gaussian decay around each station, with a decay rate determined by the spatial spread. The areal estimates of the Moho surface for the Alice Springs to Mount Isa region have been extracted on a 0.25° grid (Figure 2).

**Table 1. Weighting and spatial spread of Moho estimates used in Moho surface construction**

	<i>Relative Weighting</i>	<i>Spatial Spread (°)</i>
Refraction	0.6	1.2
Reflection	0.9	0.2
Receiver Functions	1.0	0.6
Autocorrelation	0.9	0.5
Tomography	0.9	0.6

### RESULTS

Here we present new results with an updated Moho surface in the Alice Springs to Mount Isa region, which spans a major part of the North Australian Craton (Schofield *et al.*, 2020). To the south, the region transects the northern boundary of the South Australian Craton, and, to the east, the region links into the Paleozoic Tasman Fold Belt, but in many places the transition is obscured by sedimentary cover. Prior data coverage of the region was limited, with a modest number of portable seismic stations, and a more developed network of reflection profiles in the east (Kennett *et al.*, 2016). The deployment of portable seismic stations under the Exploring for the Future program linked previous deployments and provides a regular coverage over this region (Figure 1; Gorbatov *et al.*, 2020). The new reflection profiles extend to the west and northwest from the exposures of the Paleo- to Mesoproterozoic Mount Isa Province into the regions obscured by surface cover (Fomin *et al.*, 2020).

The Moho surface in Figure 2 has significant contrasts in the thickness of the crust, from 27 km (e.g. around the southern coastline of the Gulf of Carpentaria) to more than 50 km in the southern part of the exposed Mount Isa Province and in the northern part of the Macarthur Basin. The surface construction technique uses Gaussian decay functions and, as a result, relative rapid variations in Moho depth are preserved (Kennett, 2019). Gravimetric measurements independently confirm the correctness of derived Moho shape at long wavelengths. With the complex variation in the geometry of the Moho estimates

and their physical character, there is competition between the broad-scale and smaller-scale aspects of the behaviour, so resolution is not uniform across the region. However, the broad-scale behaviour is consistent with earlier continental scale Moho results (e.g. Salmon et al., 2013), but the increased coverage provides much more detail.

Migrated image analysis that projects seismic rays on vertical cross-sections clearly images sharp changes in the depth to Moho. There is no simple relation between the depth to Moho and major tectonic boundaries, but there is a tendency for zones with Proterozoic basement to be related with zones of thicker crust. Our results reveal sharp steps in Moho depth of ~10 km at ~100 km wavelengths. Some of these steps can be easily associated with major known structure such as the Willowra Suture. In other areas, undulations in Moho depth correspond to areas of sedimentary cover and may indicate the presence of previously unknown major structures.

Inspection of the Moho surface and the spatial distribution of iron oxide–copper–gold and sedimentary hosted lead, zinc and copper deposits suggests that significant deposits (>2 Mt) are distributed along the edges of second-order north–south to northeast–southwest-trending thicker crustal blocks (Figure 2). Potential exceptions may include deposits around Mount Isa and Cannington, but close inspection of constraints adjacent to these deposits indicates that the Moho grid underrepresented variations in these areas. Since the distribution of these deposits has been shown to align along the edges of thick lithosphere (Hoggard et al., 2020), the intersection of these two seismologically defined trends may prove to be a fruitful targeting criterion. Higher-resolution seismic surveys would be useful to further test the mineral systems implications of these observations.

## CONCLUSIONS

High resolution Moho discontinuity models can assist in identification of crustal structures hidden under cover. Initial analysis of iron oxide–copper–gold and sedimentary hosted lead, zinc and copper deposit distribution suggests that they tend to be located in areas associated with strong undulations in the depth to Moho. Further studies are required to establish robust relationship between Moho features and nature of mineral deposit distribution. These studies can be facilitated by accessing the Exploring for the Future portal <https://portal.ga.gov.au/persona/efrf> where models are stored for easy access and further analysis in both 2D and 3D.

## ACKNOWLEDGMENTS

This abstract is published with the permission of the CEO of Geoscience Australia. We thank reviewers Adrian Hitchman and Leigh Franks for their corrections and suggestions, Jason Zhao and Josef Holzschuh for their contribution to AusArray program. We acknowledge all landholders, communities and traditional custodians who have supported our work in rural, regional and remote Australia.

## REFERENCES

Ammon, C. J., 1991. The isolation of receiver effects from teleseismic P waveforms, *Bull. Seism. Soc. Am.*, 81, 2504–2510.

Fomin T., Holzschuh J., Costelloe R. D., Henson P., 2020. Northern Australia 2D deep reflection seismic surveys. In: Czarnota K., et al. (eds.), *Exploring for the Future: extended abstracts*, Geoscience Australia, Canberra, 1–4

Hassan R., Hejrani B., Medlin A., Gorbatov A. & Zhang F., 2020. High-performance seismological tools (HiPerSeis). In: Czarnota K., et al. (eds.), *Exploring for the Future: extended abstracts*, Geoscience Australia, Canberra, 1–4. <http://dx.doi.org/10.11636/135095>

Hoggard, M. J., Czarnota, K., Richards, F. D., Huston, D. L., Jaques, L. & Ghelichkhan, S., 2020. Global distribution of sediment-hosted metals controlled by craton edge stability. *Nature Geoscience* 13, 504–510. <https://doi.org/10.1038/s41561-020-0593-2>

Kennett B. L. N., 2019, Areal parameter estimates from multiple datasets. *Proceedings of the Royal Society A*, 475:20190352. <https://doi.org/10.1098/rspa.2019.0352>

Kennett B. L. N., Saygin E., Fomin T. & Blewett R. S., 2016, Deep crustal seismic reflection profiling Australia 1978–2015, ANU Press, Canberra.

Kosarev G. Kind R. Sobolev S.V. Yuan X. Hanka W. Oreshin S., 1999, Seismic evidence for a detached Indian lithospheric mantle beneath Tibet, *Science*, 283, 1306–1309. <https://doi.org/10.1126/science.283.5406.1306>

Qashqai T. M., Saygin E. & Kennett B. L. N., 2019, Crustal imaging with Bayesian inversion of teleseismic P-wave coda autocorrelation. *Journal of Geophysical Research: Solid Earth* 124:5888–906. <https://doi.org/10.1029/2018JB017055>

Salmon M., Kennett B. L. N., Stern T. & Aitken A. R. A., 2013. The Moho in Australia and New Zealand. *Tectonophysics*, 609:288–98. <https://doi.org/10.1016/j.tecto.2012.07.009>

Skirrow R. G., et al. 2019. Mapping iron oxide Cu-Au (IOCG) mineral potential in Australia using a knowledge-driven mineral systems-based approach. *Ore Geology Reviews* 113:103001.

Tkalčić, H., Chen, Y., Liu, R., Zhibin, H., Sun, L. and Chan, W., 2011, Multistep modelling of teleseismic receiver functions combined with constraints from seismic tomography: crustal structure beneath southeast China. *Geophysical Journal International*, 187: 303–326. <https://doi.org/10.1111/j.1365-246X.2011.05132.x>.

Yu, Y., Song, J., Liu, K. H., and Gao, S. S., 2015, Determining crustal structure beneath seismic stations overlying a low-velocity sedimentary layer using receiver functions. *J. Geophys. Res. Solid Earth*, 120, 3208–3218. <https://doi.org/10.1002/2014JB011610>.

Zhu, L., and Kanamori H., 2000, Moho depth variation in Southern California from teleseismic receiver functions, *J. Geophys. Res.*, 105, 2969–2980. <https://doi.org/10.1029/1999JB900322>.

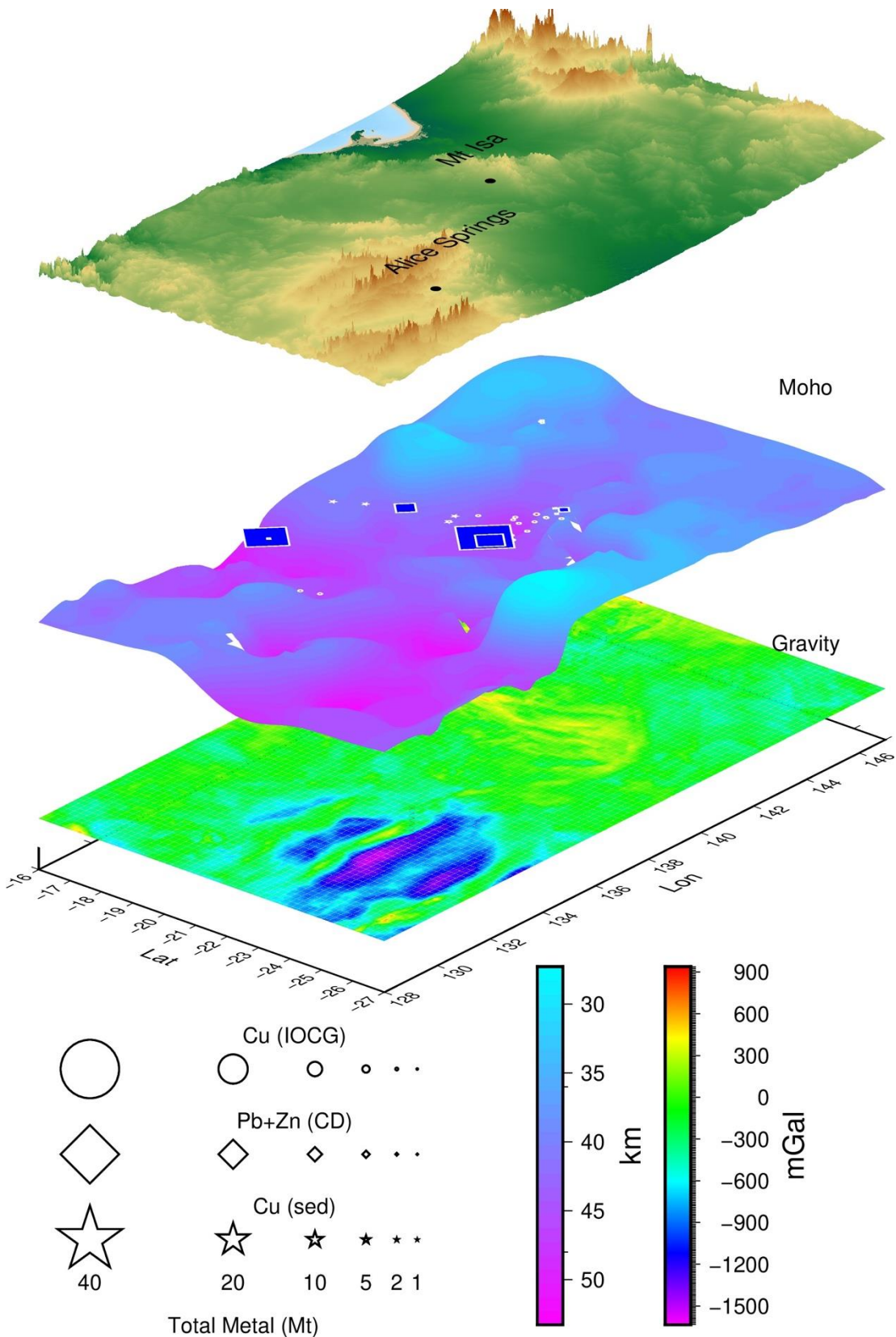


Figure 2. Configuration of the depth to Moho discontinuity (middle), topography (top) and gravity anomalies (bottom). Major mineral deposits are overlain on the Moho surface. Note that most deposits are located above changes in crustal thickness. Deposit type abbreviations: IOCG = iron oxide-copper-gold; Pb+Zn (CD) = sediment hosted clastic dominated lead and zinc; Cu (sed) = sediment-hosted copper deposits (Hoggard et al., 2020).